

12

AD-A274 346



Prewhitening of Colored Noise Fields For Detection of Threshold Sources

Alain C. Barthelemy
Submarine Sonar Department

DTIC
ELECTE
JAN 0 8 1994
S B D



93-31481



Naval Undersea Warfare Center Detachment
New London, Connecticut

**Best
Available
Copy**

PREFACE

This report was prepared under Project No. 710C10, *Computationally Efficient Algorithms for Subspace Estimation*, principal investigator Alain C. Barthelemy, Code 2151, NUWC Detachment New London.

The technical reviewer for this report was R. R. Kneipfer, Code 214, NUWC Detachment New London.

The author is grateful to Dr. W. I. Roderick for his funding of the original project, T. C. Choinski and M. H. Leonhardt for their guidance and encouragement during the preparation of the manuscript, and Dr. N. L. Owsley of NUWC Detachment New London and Dr. P. K. Willett from the University of Connecticut for their significant contributions to the research.

REVIEWED AND APPROVED: 7 NOVEMBER 1993


F. J. Kingsbury
Head, Submarine Sonar Department

REPORT DOCUMENTATION PAGE

Form Approved
OMB No. 0704-0188

Public reporting burden for this collection of information is estimated to average 1 hour per response, including the time for reviewing instructions, searching existing data sources, gathering and maintaining the data needed, and completing and reviewing the collection of information. Send comments regarding this burden estimate or any other aspect of this collection of information, including suggestions for reducing this burden, to Washington Headquarters Services, Directorate for Information Operations and Reports, 1215 Jefferson Davis Highway, Suite 1204, Arlington, VA 22202-4302, and to the Office of Management and Budget, Paperwork Reduction Project (0704-0188), Washington, DC 20503.

1. AGENCY USE ONLY (Leave Blank)		2. REPORT DATE 7 November 1993	3. REPORT TYPE AND DATES COVERED FINAL	
4. TITLE AND SUBTITLE Prewhitening of Colored Noise Fields for Detection of Threshold Sources			5. FUNDING NUMBERS	
6. AUTHOR(S) Alain C. Barthelemy				
7. PERFORMING ORGANIZATION NAME(S) AND ADDRESS(ES) Naval Undersea Warfare Center Detachment New London New London, Connecticut 06320			8. PERFORMING ORGANIZATION REPORT NUMBER TR 10,495	
9. SPONSORING/MONITORING AGENCY NAME(S) AND ADDRESS(ES)			10. SPONSORING/MONITORING AGENCY REPORT NUMBER	
11. SUPPLEMENTARY NOTES				
12a. DISTRIBUTION/AVAILABILITY STATEMENT Approved for public release; distribution is unlimited.			12b. DISTRIBUTION CODE	
13. ABSTRACT (Maximum 200 words) <p>This report presents an algorithm for the estimation of noise correlations for an array of sensors. The algorithm assumes a mixed spectra model composed of discrete sinusoidal sources and continuous noise components. A spatial AR process models the continuous component. Previous methods use spatial AR models with real coefficients, restricting the utility of the model to noise sources that impinge on an array at broadside. The complex formulation presented here solves the general problem of arbitrarily oriented noise sources. The technique uses a gradient algorithm for maximization of a likelihood functional to solve for the complex AR coefficients.</p> <p>Once the algorithm determines the noise covariance matrix, prewhitening techniques allow detection of threshold sources. The multiple signal classification (MUSIC) direction finder when applied to the prewhitened observed correlation matrix illustrates the usefulness in detecting low signal-to-noise ratio (SNR) sources.</p> <p>Computational examples used the standardized test case (STC), a realistic model with a challenging range of SNR and difficult source locations.</p>				
14. SUBJECT TERMS AR Model, Colored Noise Field, Mixed Spectra Model, MUSIC, Noise Field, Prewhitening, SNR, Standardized Test Case, Threshold Sources			15. NUMBER OF PAGES 52	
			16. PRICE CODE	
17. SECURITY CLASSIFICATION OF REPORT UNCLASSIFIED	18. SECURITY CLASSIFICATION OF THIS PAGE UNCLASSIFIED	19. SECURITY CLASSIFICATION OF ABSTRACT UNCLASSIFIED	20. LIMITATION OF ABSTRACT SAR	

TABLE OF CONTENTS

LIST OF ILLUSTRATIONS	ii
LIST OF TABLES	ii
LIST OF ACRONYMS, ABBREVIATIONS, AND SYMBOLS	ii
INTRODUCTION	1
MOTIVATION FOR PREWHITENING	3
EXAMPLE 1: EXTENDED SOURCE ENERGY SPECTRUM	4
EXAMPLE 2: COMPLEX AR COEFFICIENT	5
EXAMPLE 3: MUSIC IN A COLORED BACKGROUND NOISE	6
METHOD OF PREWHITENING	9
THE LIKELIHOOD FUNCTIONAL	10
MAXIMIZATION OF THE LIKELIHOOD FUNCTIONAL -	
LE CADRE'S TECHNIQUE	12
EXAMPLE 4: LIKELIHOOD FUNCTIONAL SURFACE CONTOUR	13
LEMMAS: EIGENVALUES OF PREWHITENED COVARIANCE MATRIX	14
ALGORITHM FOR MAXIMIZATION OF THE LIKELIHOOD FUNCTIONAL	15
PERFORMANCE METRICS	17
THE STC SIMULATIONAL DATA	18
RESULTS OF SIMULATION	19
CONCLUSIONS	25
APPENDIX A: COMPUTATION OF $\partial Q^{-1} / \partial a_i$	A-1
APPENDIX B: SOURCE CODE FOR PREWHITENING ALGORITHM	B-1
REFERENCES	R-1

DTIC QUALITY INSPECTED 6

Accession For	
NTIS GRA&I	<input checked="" type="checkbox"/>
DTIC TAB	<input type="checkbox"/>
Unannounced	<input type="checkbox"/>
Justification	
By _____	
Distribution/	
Availability Codes	
Dist.	Avail and/or Special
A-1	

LIST OF ILLUSTRATIONS

Figure		Page
1	Extended Source Spectrum.....	4
2	Pole Plot for Example 2.....	6
3	MUSIC Spectra for Example 3.....	7
4	Relation of Likelihood Functional to ARMA Parameters.....	13
5	Maximization Surface Contour Plot of $L_q(Q)$	13
6	The STC.....	18
7	Pole Plot for STC.....	20
8	Cosine Metric for STC.....	20
9	Noise Spatial Density for STC.....	21
10	MUSIC Response for STC.....	21
11	Eigenvalues of the STC.....	22
12	Likelihood Functional Surface for STC.....	23
13	Likelihood Functional Contour for STC.....	24

LIST OF TABLES

Table		Page
1	The Standardized Test Case (STC).....	18
2	Values of Likelihood Functional for Standardized Test Case (STC).....	22

LIST OF ACRONYMS, ABBREVIATIONS, AND SYMBOLS

SNR	Signal-to-Noise Ratio
ARMA	Autoregressive Moving Average
AR	Autoregressive
STC	Standardized Test Case
MUSIC	Multiple Signal Classification
ESPRIT	Estimation of Signal Parameters Via Rotational Invariance Techniques
PHD	Pisarenko Harmonic Decomposition

EMVDR	Enhanced Minimum Variance Distortionless Response
dB	Decibel
DOA	Direction of Arrival
DS	Discrete Source
ES	Extended Source
A	Matrix
a	Vector
a	Scalar
N	Number of Array Sensors
L	Order of AR Model
q	Estimated Number of Discrete Sources
P	Estimated Number of Extended Sources
d	Nominal Spacing Between Sensors
k	Snapshot Index
()_k or ()^k	k-th Iteration
K	Total Number of Snapshots
I_N	N by N Identity Matrix
0_N	N by N Zero Matrix
j	Indication of a Complex Number, $j = \sqrt{-1}$

PREWHITENING OF COLORED NOISE FIELDS FOR DETECTION OF THRESHOLD SOURCES

INTRODUCTION

High resolution direction finding methods such as Multiple Signal Classification (MUSIC),¹ Enhanced Minimum Variance Distortionless Response (EMVDR),² and Minimum Norm (Min-Norm)³ compute angular response as a function of cosine of bearing angle. These methods associate peaks in the response function with source locations, providing direction of arrival estimates. A response peak that does not correspond to an existing source indicates a false alarm. Rooting techniques for direction finding such as ROOT-MUSIC,⁴ Estimation of Signal Parameters Via Rotational Invariance Techniques (ESPRIT),⁵ and the Pisarenko Harmonic Decomposition (PHD)⁶ provide source locations directly, without computation of a response function, by constructing a polynomial whose roots correspond to arrival angles. Any angle that does not correspond to an existing source indicates a false alarm. Typically, these algorithms provide a large set of candidate arrival angles that includes true source locations and spurious ones. Although methods exist for determining the true source locations from the candidate set,⁷ they require an accurate set of candidate angles with as few false alarms as possible.

Both types of direction finders exhibit high false alarm rates in the presence of spatially colored ambient noise. In their traditional model formulation, direction finders assume that only spatially white noise exists. When an extended or continuous colored noise is present in the acoustic field, low SNR or threshold sources may be obscured from detection. Also, the estimate of a source location for a source that exists within the spatial bandwidth of the colored noise may be biased. Thus, in the presence of known nonwhite noise, high false alarm performance necessitates the use of prewhitening algorithms.⁸ Direction finders also require a reliable estimate of the number of sources present in the observed noise field.⁸ Because nonwhite noise skews or inflates this estimate, prewhitening is required.

MOTIVATION FOR PREWHITENING

Define \mathbf{x} as the N -dimensional sensor output data vector from an N -element uniform line array. Denote the covariance matrix of \mathbf{x} by

$$\mathbf{R} = E[\mathbf{x}\mathbf{x}^H], \quad (1)$$

where

$$\mathbf{x}^T = [x_1 \ x_2 \ \dots \ x_N], \quad (2)$$

$E[\]$ represents the expectation operator, and H denotes complex conjugate transpose. Model \mathbf{R} with the following structure⁹

$$\mathbf{R} = \sigma_{DS}^2 \mathbf{P} + \sigma_{ES}^2 \mathbf{Q} + \sigma_0^2 \mathbf{I}_N, \quad (3)$$

where \mathbf{P} corresponds to the discrete source (DS) component, \mathbf{Q} to the extended source (ES) component (in this case colored noise), and \mathbf{I}_N (an N by N identity matrix) to the component due to uncorrelated noise. Normalize \mathbf{P} and \mathbf{Q} so that each trace equals N . The three variances, σ_{DS}^2 , σ_{ES}^2 , and σ_0^2 , represent the power at a single sensor due to discrete sources, extended sources, and uncorrelated noise, respectively.

Define the discrete source component \mathbf{P} corresponding to $q \leq N$ discrete angular sources at θ_i , $i = 1, 2, \dots, q$, as⁹

$$\mathbf{P} = \mathbf{D}\mathbf{C}\mathbf{D}^H, \quad (4)$$

where the N by q steering matrix $\mathbf{D} = [\mathbf{d}_1 \ \mathbf{d}_2 \ \dots \ \mathbf{d}_q]$ contains the i -th column

$$\mathbf{d}_i^T = [1 \ e^{-j\mathbf{k}_i d} \ e^{-j\mathbf{k}_i (2d)} \ \dots \ e^{-j\mathbf{k}_i (N-1)d}], \quad (5)$$

and the wavenumber of the i -th source at θ_i is

$$\mathbf{k}_i = \frac{2\pi}{\lambda} \cos(\theta_i). \quad (6)$$

The factor d is the nominal spacing between sensors, given as a fraction of the wavelength λ . Write the above expression as a function of angular frequency equal to the cosine of the bearing angle of interest θ , with $0 \leq \theta \leq \pi$. Assume a diagonal source coherence matrix C so that no correlation exists between sources. A thin spike or delta function illustrates the spatial density of a discrete source at bearing angle θ .

EXAMPLE 1: EXTENDED SOURCE ENERGY SPECTRUM

The angular energy spectrum of an extended source at bearing angle θ affects a spatial bandwidth around the angle θ .

Compute the spatial density of an arbitrary extended source modeled as a first order autoregressive (AR) process with coefficient $a_1 = -0.7$ steered to 45 degrees. Figure 1 depicts the spatial density.

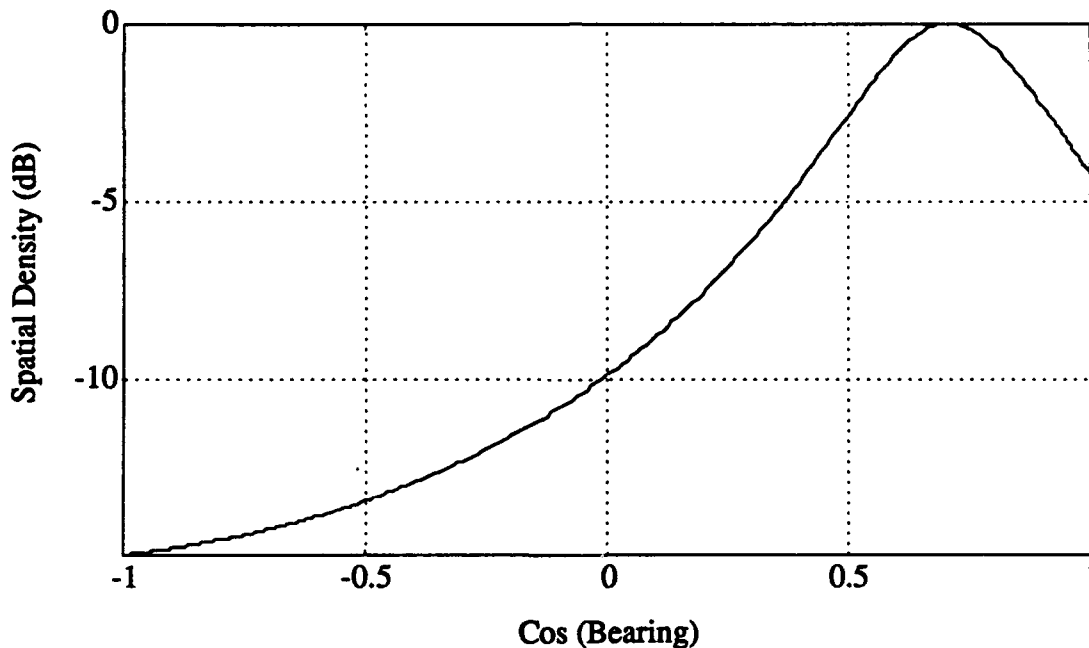


Figure 1. Extended Source Spectrum

Model the P extended sources in component Q as the sum of L -th order AR spatial processes Q_i utilizing the Gohberg Formula¹⁰ with complex coefficients $a_{i,j}$, scaled by a factor α_i , $i = 1, 2, \dots, P$, as follows:

$$\theta = 45 \text{ degrees ,} \quad (13)$$

and

$$\begin{aligned} \tilde{a}_1 &= -0.7e^{j2\pi(0.25)\cos(45)} \\ &= -0.3108 - 0.6272i . \end{aligned} \quad (14)$$

While figure 1 has illustrated the spatial energy density for this process, figure 2 shows a pole plot of the coefficient \tilde{a}_1 .

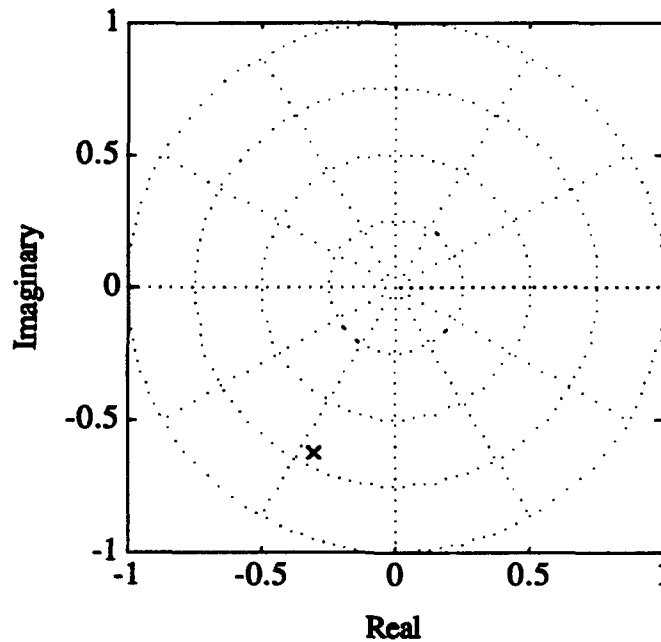


Figure 2. Pole Plot for Example 2

EXAMPLE 3: MUSIC IN A COLORED BACKGROUND NOISE

Now, consider an example that illustrates the degradation in performance when the MUSIC direction finder is used in a nonwhite background spectrum environment.

Given an eight sensor array with quarter-wavelength sensor spacing and a 0-dB extended source from example 2, inject two discrete sources into the observed noise field:

Discrete source 1: 30 degrees, SNR = -3 dB

Discrete source 2: 70 degrees, SNR = -19 dB.

Compare the MUSIC spectra for the prewhitened and non-prewhitened cases. For the MUSIC computation, assume the presence of $q = 3$ sources.

In figure 3, the dotted vertical lines represent the true direction of arrival (DOA) angles. The dashed line corresponds to the prewhitened MUSIC spectra. The non-prewhitened case exhibits a strong bias due to the extended source at 45 degrees. The stronger extended source obscures the low SNR source at 70 degrees.

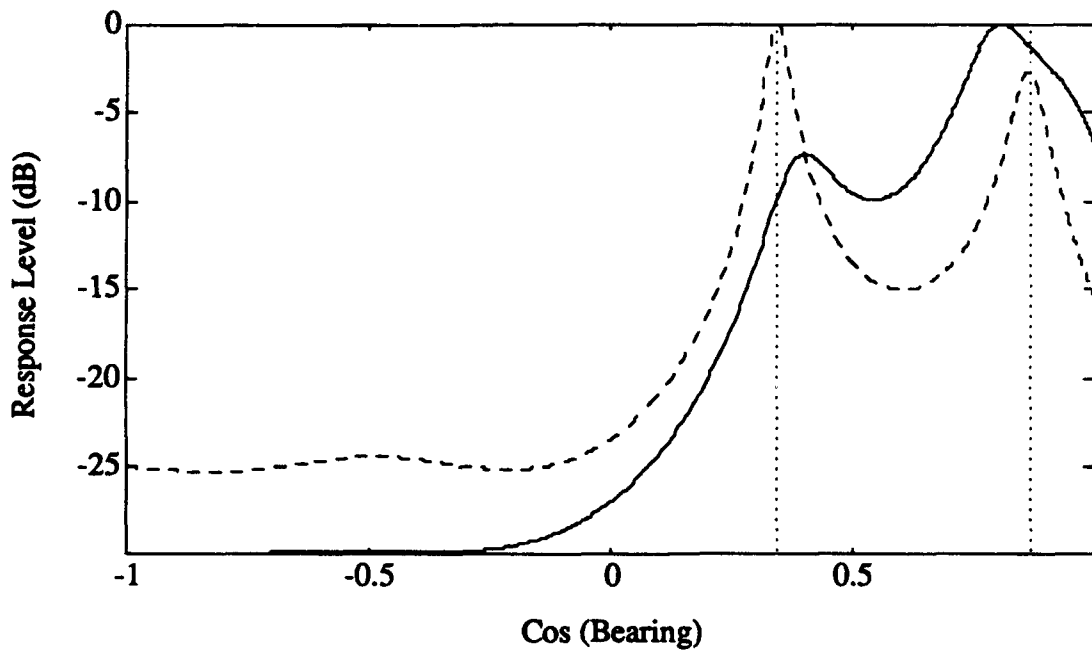


Figure 3. MUSIC Spectra for Example 3

METHOD OF PREWHITENING

Define $\tilde{\mathbf{x}}$ as an N-dimensional vector whose covariance matrix is given by

$$\begin{aligned}\tilde{\mathbf{R}} &= E[\tilde{\mathbf{x}}\tilde{\mathbf{x}}^H] \\ &= \mathbf{R} - \sigma_0^2 \mathbf{I}_N \\ &= \sigma_{DS}^2 \mathbf{P} + \sigma_{ES}^2 \mathbf{Q},\end{aligned}\tag{15}$$

where $\tilde{\mathbf{x}} = [\tilde{x}_1 \ \tilde{x}_2 \ \dots \ \tilde{x}_N]^T$. Note that $\tilde{\mathbf{R}}$ is the covariance matrix in the absence of uncorrelated noise and can be estimated by using the smallest eigenvalue of \mathbf{R} as an estimate of σ_0^2 .

If \mathbf{L}_{ES} is the lower triangular matrix Cholesky factor given by

$$\mathbf{L}_{ES} \mathbf{L}_{ES}^H = \sigma_{ES}^2 \mathbf{Q},\tag{16}$$

define a prewhitened snapshot vector as

$$\mathbf{x}_{PW} = \mathbf{L}_{ES}^{-1} \tilde{\mathbf{x}}.\tag{17}$$

The covariance matrix \mathbf{R}_{PW} of the prewhitened vector then contains a purely white spatial noise density,

$$\begin{aligned}\mathbf{R}_{PW} &= E[\mathbf{x}_{PW} \mathbf{x}_{PW}^H] \\ &= \mathbf{L}_{ES}^{-1} \tilde{\mathbf{R}} \mathbf{L}_{ES}^{-H} \\ &= \sigma_{DS}^2 \mathbf{L}_{ES}^{-1} \mathbf{P} \mathbf{L}_{ES}^{-H} + \sigma_{ES}^2 \mathbf{L}_{ES}^{-1} \mathbf{Q} \mathbf{L}_{ES}^{-H} \\ &= \sigma_{DS}^2 \mathbf{L}_{ES}^{-1} \mathbf{P} \mathbf{L}_{ES}^{-H} + \sigma_{ES}^2 \mathbf{L}_{ES}^{-1} \frac{\mathbf{L}_{ES} \mathbf{L}_{ES}^H}{\sigma_{ES}^2} \mathbf{L}_{ES}^{-H} \\ &= \sigma_{DS}^2 \mathbf{L}_{ES}^{-1} \mathbf{P} \mathbf{L}_{ES}^{-H} + \mathbf{I}_N,\end{aligned}\tag{18}$$

where

$$\mathbf{L}_{ES}^{-H} = (\mathbf{L}_{ES}^H)^{-1}.\tag{19}$$

The algorithm for prewhitening the measured matrix $\tilde{\mathbf{R}}$ minimizes a likelihood functional¹¹ to obtain an estimate of \mathbf{Q} .

THE LIKELIHOOD FUNCTIONAL

Following the development in reference (11), assume we are given K array data snapshots in a sequence,

$$\{\mathbf{x}_1, \mathbf{x}_2, \dots, \mathbf{x}_K\}, \quad (20)$$

with covariance \mathbf{R} . Form the estimate¹² of \mathbf{R} as

$$\hat{\mathbf{R}} = \frac{1}{K} \sum_{k=0}^{K-1} \mathbf{x}_k \mathbf{x}_k^H. \quad (21)$$

The likelihood functional relates the estimate $\hat{\mathbf{R}}$ to an assumed covariance structure \mathbf{R} . To aid in the derivation, first assume that the true covariance

$$\mathbf{R} = \mathbf{P} + \lambda \mathbf{I}_N \quad (22)$$

corresponds to the white noise case, and omit the scale factors for brevity. The factor λ equals a positive scalar parameter. The matrix \mathbf{P} equals an unknown covariance matrix of rank q . Although methods¹³⁻¹⁵ exist for the computation of q , the number of sources present assume that q represents a known quantity. The function

$$f(\{\mathbf{x}_1, \mathbf{x}_2, \dots, \mathbf{x}_K\} / \lambda, \mathbf{P}) = \frac{1}{\pi^{KN} |\mathbf{R}|^K} e^{-K \text{trace}(\tilde{\mathbf{R}} \mathbf{R}^{-1})} \quad (23)$$

represents the conditional density for the complex Gaussian sequence \mathbf{x}_i , $i = 1, 2, \dots, K$, with covariance \mathbf{R} conditioned on (λ, \mathbf{P}) and $||$ being the determinant operator. The function $\text{trace}(\mathbf{A})$ sums the diagonal elements of matrix \mathbf{A} . The problem now involves seeking the values for (λ, \mathbf{P}) that maximize this likelihood. To express the log-likelihood as a functional in terms of the eigenvalues of $\hat{\mathbf{R}}$, $\hat{\lambda}_1 \geq \hat{\lambda}_2 \geq \dots \geq \hat{\lambda}_N$, define

$$\bar{\lambda}_{GM}(q) = \left(\prod_{i=q+1}^N \hat{\lambda}_i \right)^{\frac{1}{N-q}} \quad (24)$$

and

$$\bar{\lambda}_{AM}(q) = \frac{1}{N-q} \left(\sum_{i=q+1}^N \hat{\lambda}_i \right) \quad (25)$$

as the geometric and arithmetic means, respectively, of the $N-q$ lowest eigenvalues of $\hat{\mathbf{R}}$. As shown in reference (11), we can then write

$$\begin{aligned} & \max \ln(f(\{\mathbf{x}_1, \mathbf{x}_2, \dots, \mathbf{x}_K\} / \lambda, \mathbf{P})) \\ & = K \left(-N \ln(\pi) - N - \ln(|\hat{\mathbf{R}}|) + \sum_{i=q+1}^N \ln(\hat{\lambda}_i) - (N-q) \ln(\bar{\lambda}_{AM}(q)) \right). \end{aligned} \quad (26)$$

Maximizing the likelihood is equivalent to maximizing the functional:

$$L_q(\mathbf{Q}) = (N-q) \left(\ln(\bar{\lambda}_{GM}(q)) - \ln(\bar{\lambda}_{AM}(q)) \right). \quad (27)$$

For the spatially nonwhite case, use the form

$$\tilde{\mathbf{R}} = \mathbf{P} + \lambda \mathbf{Q} \quad (28)$$

for the assumed true covariance matrix. As in the preceding section, decompose \mathbf{Q} into Cholesky triangular factors,

$$\mathbf{Q} = \mathbf{L}\mathbf{L}^H, \quad (29)$$

and form the prewhitened covariance matrix

$$\mathbf{R}_{PW} = \mathbf{L}^{-1} \tilde{\mathbf{R}} \mathbf{L}^{-H}. \quad (30)$$

It can then be shown (see reference (11)) that the likelihood functional conditional to the noise covariance \mathbf{Q} with q sources is

$$L_q(\mathbf{Q}) = (N - q) \left(\ln \left(\bar{\lambda}_{\text{WGM}}(q) \right) - \ln \left(\bar{\lambda}_{\text{WAM}}(q) \right) \right), \quad (31)$$

where $\bar{\lambda}_{\text{WGM}}(q)$ and $\bar{\lambda}_{\text{WAM}}(q)$ correspond to the geometric and arithmetic means, respectively, of the eigenvalues of the prewhitened covariance matrix \mathbf{R}_{PW} . The geometric and arithmetic means realize equality only for the case of equality between the $N-q$ lowest eigenvalues. The equality of the $N-q$ smallest eigenvalues represents a flat, spatially white noise spectrum, and in this case, $L_q(\mathbf{Q})$ equals zero.

MAXIMIZATION OF THE LIKELIHOOD FUNCTIONAL - LE CADRE'S TECHNIQUE

The prewhitening problem next becomes one of maximizing $L_q(\mathbf{Q})$ relative to the coefficients a_1, a_2, \dots, a_L parameterizing the noise covariance matrix \mathbf{Q} . Accomplish the maximization by an iterative gradient algorithm¹¹ at step k with parameter vector

$$\mathbf{A}_k^T = (\sigma_k^2, a_1^k, a_2^k, \dots, a_L^k) \quad (32)$$

and general form

$$\mathbf{A}_{k+1} = \mathbf{A}_k - \rho_0 \mathbf{G}_k, \quad (33)$$

where ρ_0 defines a step size, in this case constant, and \mathbf{G}_k defines the gradient vector. Computation of the i -th element of \mathbf{G}_k consists of calculating

$$\mathbf{G}_k(i) = \frac{\partial}{\partial a_i^k} \lambda_j^k \quad (34)$$

for $i = 1, 2, \dots, L$. Figure 4 expresses a functional relationship between the eigenvalues of the prewhitened covariance matrix, the likelihood function, and the AR coefficients. The algorithm seeks to find the maximum of the likelihood functional surface parameterized by the AR coefficients.

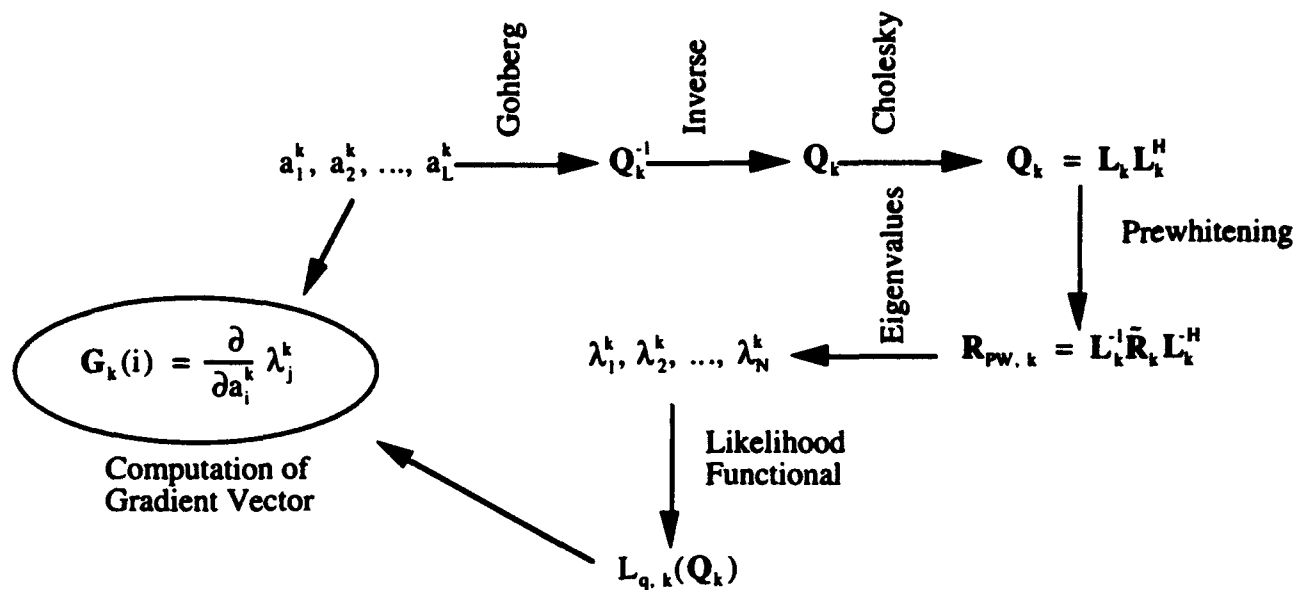


Figure 4. Relation of Likelihood Functional to ARMA parameters

EXAMPLE 4: LIKELIHOOD FUNCTIONAL SURFACE CONTOUR

Given the acoustic field from example 3, plot the maximization surface contour of $L_q(\mathbf{Q})$ in figure 5 as a function of the real and imaginary parts of the coefficient \tilde{a}_1 .

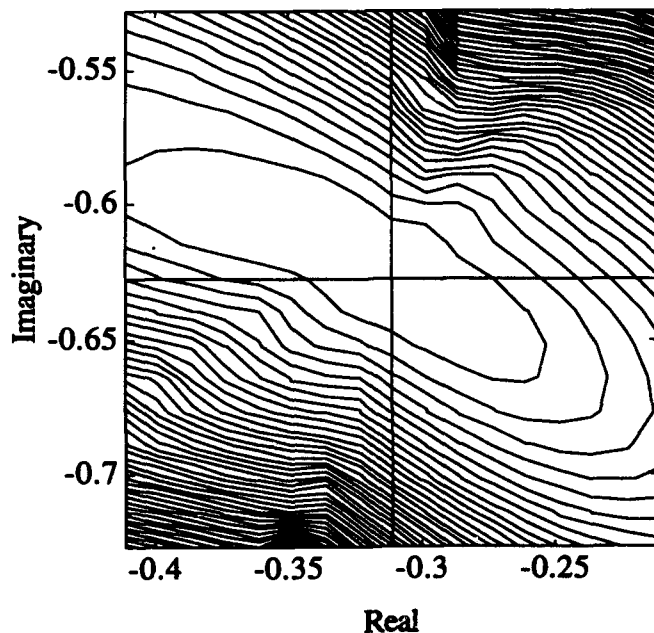


Figure 5. Maximization Surface Contour Plot of $L_q(\mathbf{Q})$

Clearly, the maximum value of $L_q(\mathbf{Q})$ occurs at the exact value of the coefficient computed in example 2.

Computation of the gradient vector reduces to

$$\mathbf{G}_k(i) = \frac{\partial}{\partial a_i^k} \lambda_j^k \quad (35)$$

for $i = 1, 2, \dots, L$ and $j = 1, 2, \dots, N$.

LEMMAS: EIGENVALUES OF PREWHITENED COVARIANCE MATRIX

The following lemmas represent intermediate steps in this computation.

Lemma 1: The eigenvalues of $\mathbf{R}_{pw,k}$ equal the eigenvalues of $\mathbf{Q}_k^{-1}\hat{\mathbf{R}}$.

Proof: To compute the eigenvalues $\lambda_1, \lambda_2, \dots, \lambda_N$ of the N by N matrix \mathbf{A} , solve

$$|\mathbf{A} - \lambda\mathbf{I}_N| = 0. \quad (36)$$

With this fact and defining

$$\mathbf{L}_k\mathbf{L}_k^H = \mathbf{Q}_k^{-1}, \quad (37)$$

then

$$\begin{aligned} & |\mathbf{Q}_k^{-1}\hat{\mathbf{R}} - \lambda\mathbf{I}_N| \\ &= |\mathbf{L}_k\mathbf{L}_k^H\hat{\mathbf{R}} - \lambda\mathbf{I}_N| \\ &= |\mathbf{L}_k^H\hat{\mathbf{R}}\mathbf{L}_k - \lambda\mathbf{I}_N| \\ &= |\mathbf{R}_{pw,k} - \lambda\mathbf{I}_N|. \end{aligned} \quad (38)$$

Lemma 2: If $\hat{\mathbf{R}} = \mathbf{T}\mathbf{T}^H$, the eigenvalues of $\mathbf{R}_{pw,k}$ equal the eigenvalues of $\mathbf{T}^H\mathbf{Q}_k^{-1}\mathbf{T}$.

Proof:

$$\begin{aligned}
& |\mathbf{Q}_k^{-1} \hat{\mathbf{R}} - \lambda \mathbf{I}_N| \\
&= |\mathbf{Q}_k^{-1} \mathbf{T} \mathbf{T}^H - \lambda \mathbf{I}_N| \\
&= |\mathbf{T}^H \mathbf{Q}_k^{-1} \mathbf{T} - \lambda \mathbf{I}_N|.
\end{aligned} \tag{39}$$

Therefore the computation of $\partial \lambda_j^k / \partial a_i^k$ reduces to the computation of $\partial \mu_j^k / \partial a_i^k$, the partial derivatives of the eigenvalues of the Hermitian matrix $\mathbf{T}^H \mathbf{Q}_k^{-1} \mathbf{T}$. Since the AR coefficients form an explicit function for \mathbf{Q}_k^{-1} , this reduction represents an important result.¹¹ Additionally, use the following classical result for an N by N Hermitian matrix \mathbf{A} ($\mathbf{A} = \mathbf{A}^H$) with simple eigenvalues λ_j and associated eigenvectors \mathbf{v}_j :

$$\frac{\partial}{\partial a_i} \lambda_j = \mathbf{v}_j^H \frac{\partial}{\partial a_i} \mathbf{A} \mathbf{v}_j. \tag{40}$$

Equation (40) derives from the eigenstructure definition

$$\mathbf{A} = \sum_{j=1}^N \mathbf{v}_j \lambda_j \mathbf{v}_j^H. \tag{41}$$

ALGORITHM FOR MAXIMIZATION OF THE LIKELIHOOD FUNCTIONAL BY COMPUTATION OF THE GRADIENT VECTOR \mathbf{G}_k

Continuing to parallel the development in reference (11), we employ the above definitions and lemmas to write the algorithm as follows.

1. Compute partial derivatives of \mathbf{Q}_k^{-1} relative to the complex AR parameters a_i :

$$\Delta_i^k = \frac{\partial \mathbf{Q}_k^{-1}}{\partial a_i} = \frac{2}{\sigma_{ES}^2} (\mathbf{A}_{1,k}(\mathbf{Z}^i)^T - \mathbf{A}_{3,k}(\mathbf{Z}^{N-i})^T) \tag{42}$$

for $i = 0, 1, \dots, L$.

(See appendix A for derivation of this expression and the definition of \mathbf{Z}^i .)

2. Compute derivative matrices:

$$\begin{aligned}\Delta_i^k &= \frac{\partial}{\partial a_i} (\mathbf{T}^H \mathbf{Q}^{-1} \mathbf{T}) \\ &= \mathbf{T}^H \Delta_i^k \mathbf{T}\end{aligned}\quad (43)$$

recalling that

$$\hat{\mathbf{R}} = \mathbf{T} \mathbf{T}^H \quad (44)$$

3. Calculate partial derivatives of the simple eigenvalues of $\mathbf{R}_{p_w, k}$:

$$\frac{\partial}{\partial a_i} \lambda_j^k = (\mathbf{u}_j^k)^H \Delta_i^k \mathbf{u}_j^k, \quad (45)$$

where \mathbf{u}_j^k represents an eigenvector associated to the eigenvalue λ_j^k of $\mathbf{T}^H \mathbf{Q}^{-1} \mathbf{T}$. Compute this eigenstructure with conventional or reduced complexity algorithms.¹⁶⁻²⁵

4. Calculate the components of the gradient vector \mathbf{G}_k :

$$\mathbf{G}_k(i) = \sum_{j=q+1}^N \left(\frac{\frac{\partial}{\partial a_i} \lambda_j^k}{\lambda_j^k} \right) - \frac{\sum_{j=q+1}^N \frac{\partial}{\partial a_i} \lambda_j^k}{\bar{\lambda}_{AM}(q)}, \quad (46)$$

where

$$\bar{\lambda}_{AM}(q) = \frac{1}{N-q} \left(\sum_{j=q+1}^N \lambda_j^k \right). \quad (47)$$

5. Select step size to ensure adequate convergence rate.

Although methods¹¹ exist for updating ρ_0 , assume a fixed step size arrived at by trial-and-error.

PERFORMANCE METRICS

Four performance metrics will be used to evaluate algorithm performance:

1. Compute a pole plot of the AR coefficients by generating one at each iteration of gradient algorithm to view convergence trajectory.
2. Compute the cosine of the angle between the estimated covariance \mathbf{Q}_{EST} and the true covariance \mathbf{Q}_{TRUE} :

$$\cos(\mathbf{Q}_{EST}, \mathbf{Q}_{TRUE}) = \frac{\text{trace}(\mathbf{Q}_{EST} \mathbf{Q}_{TRUE})}{\sqrt{\text{trace}(\mathbf{Q}_{EST} \mathbf{Q}_{EST}) \text{trace}(\mathbf{Q}_{TRUE} \mathbf{Q}_{TRUE})}} \quad (48)$$

A cosine close to 1 implies collinearity.

3. Compute the AR spatial density for estimated coefficients:

$$S(z) = \frac{1}{A(z)A^*(z)}, \quad (49)$$

where " * " corresponds to the complex conjugate and

$$A(z) = a_0 + a_1 z + a_2 z^2 + \dots + a_L z^L \quad (50)$$

$$z = e^{-j2\pi d \cos(\theta)}. \quad (51)$$

4. Compute the MUSIC^{1, 26} bearing response for prewhitened case:

$$P_{MUSIC}(\theta) = \frac{1}{\mathbf{e}^H(\theta) \left(\sum_{j=q+1}^N \mathbf{u}_j \mathbf{u}_j^H \right) \mathbf{e}(\theta)}, \quad (52)$$

where

$$\mathbf{e}^T(\theta) = [1 \ e^{j2\pi d \cos(\theta)} \ e^{j4\pi d \cos(\theta)} \ \dots \ e^{j2(N-1)\pi d \cos(\theta)}] \quad (53)$$

and u_j represents an eigenvector of the prewhitened covariance matrix R_{PW} .

THE STC SIMULATIONAL DATA

To evaluate the effectiveness of the proposed method, use the STC,⁹ a realistic model with a challenging range of SNR and difficult source locations. The STC employs quarter-wavelength sensor spacing. Figure 6 depicts the STC source locations graphically and table 1 enumerates the relative source strengths.

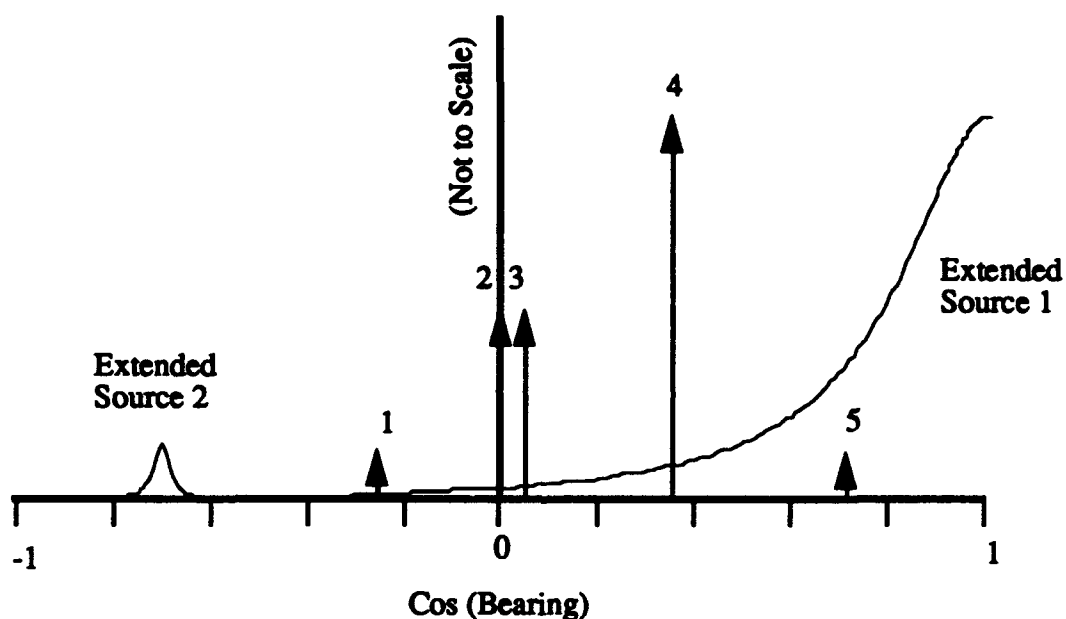


Figure 6. The STC

Table 1. The STC

	BEARING θ (DEGREES)	COS(θ)	AR PARAMETER	SNR (dB)
DISCRETE SOURCES				
1	105	-0.26	-	-20
2	90	0	-	-3
3	85	0.09	-	-3
4	70	0.34	-	0
5	45	0.71	-	-14
EXTENDED SOURCES				
1	0	1	-0.7j	0
2	135	-0.71	-0.4263+0.8602j	-27

RESULTS OF SIMULATION

Assume an $L = 4$ AR model and initialize the algorithm with parameter vector

$$\mathbf{A}^T = (1, 0, 0, 0, 0). \quad (54)$$

Run the algorithm for 25 iterations with step size $\rho_0 = -0.025$. Set q equal to the number of signal eigenvalues, 7, for the prewhitener and for MUSIC. Assume a known noise floor σ_0^2 .

Figures 7 through 10 illustrate the results of the Le Cadre algorithm on the STC. The great disparity in SNR for the two extended sources (ES) causes the algorithm to prewhiten only the noise associated with ES 1 at 0 degrees. Although a fourth-order AR process attempts to model the sum of two first order processes, in this case, a first-order model suffices. The MUSIC spectrum shows that although the prewhitening of ES 1 allows detection of the discrete source at 45 degrees, it also causes the promotion of a weak second extended source, ES 2. The number of assumed sources plays an important role in the detection of ES 2; indeed if $q = 5$, the peak at 135 degrees disappears. Attempts to prewhiten the small source at 135 degrees with a second pass of the algorithm fail because of the nature of the remaining eigenvalues of the prewhitened \mathbf{R} .

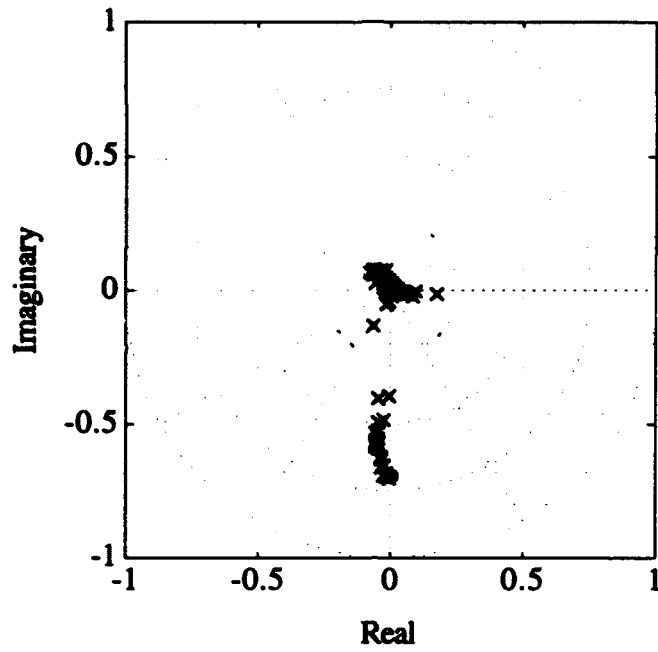


Figure 7. Pole Plot for STC

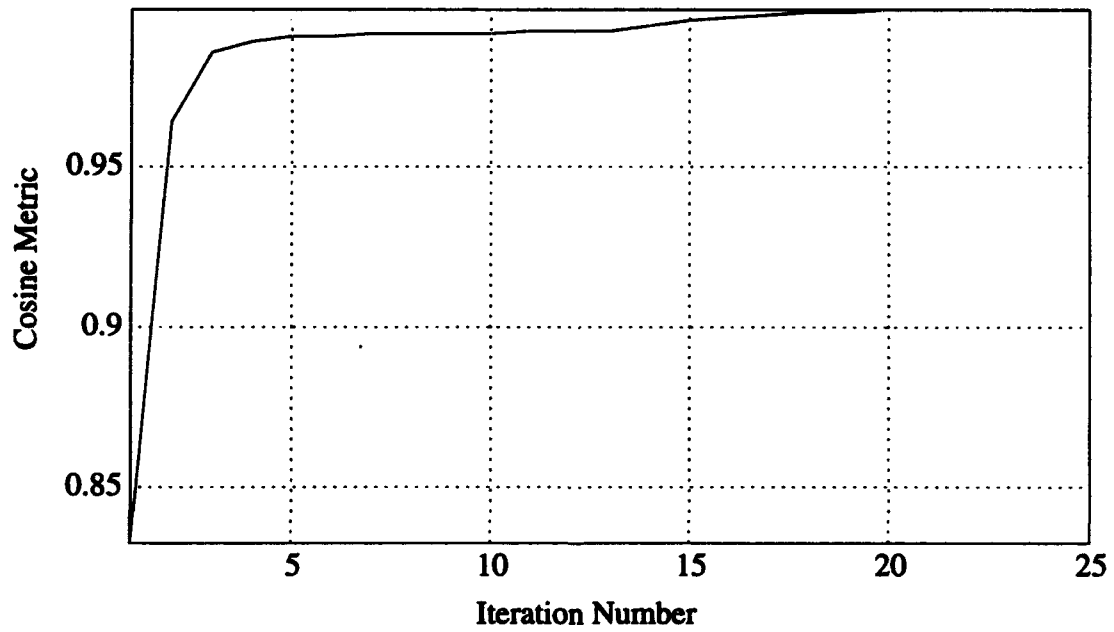


Figure 8. Cosine Metric for STC

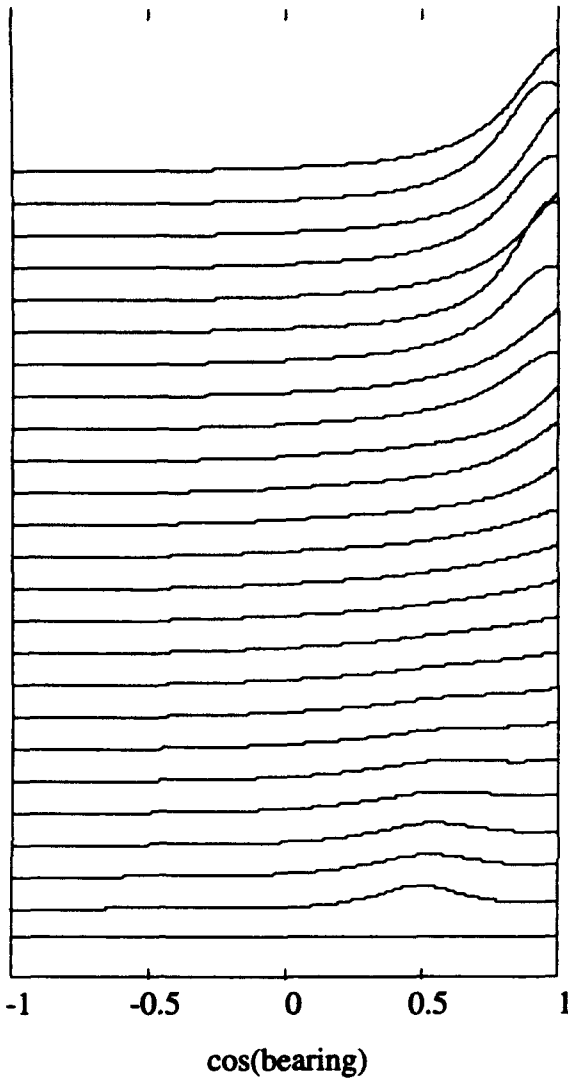


Figure 9. Noise Spatial Density for STC

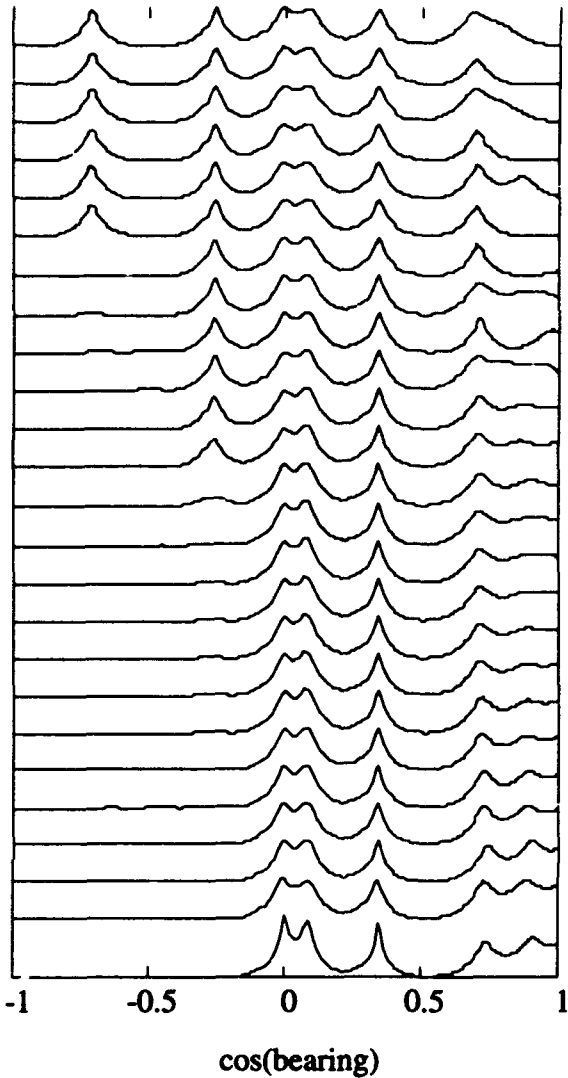


Figure 10. MUSIC Response for STC

Figure 11 depicts the eigenvalues associated with the STC. The solid line corresponds to the non-prewhitened case and the dotted line corresponds to the case following the 25th iteration of the algorithm. The dashed line represents the eigenvalues omitting the two extended sources entirely. To visualize the failure of the attempted second pass of the algorithm, recall that the likelihood functional measures the proximity of the $N-q$ ($24 - 7 = 17$) smallest eigenvalues. In this case, a comparison of these eigenvalues illustrates the algorithm difficulty. The dashed line lies so close to the dotted line that the gradients involved in the computation of the update become small relative to the step size. A flat eigenvalue spectrum corresponds to a value of zero for the likelihood functional.

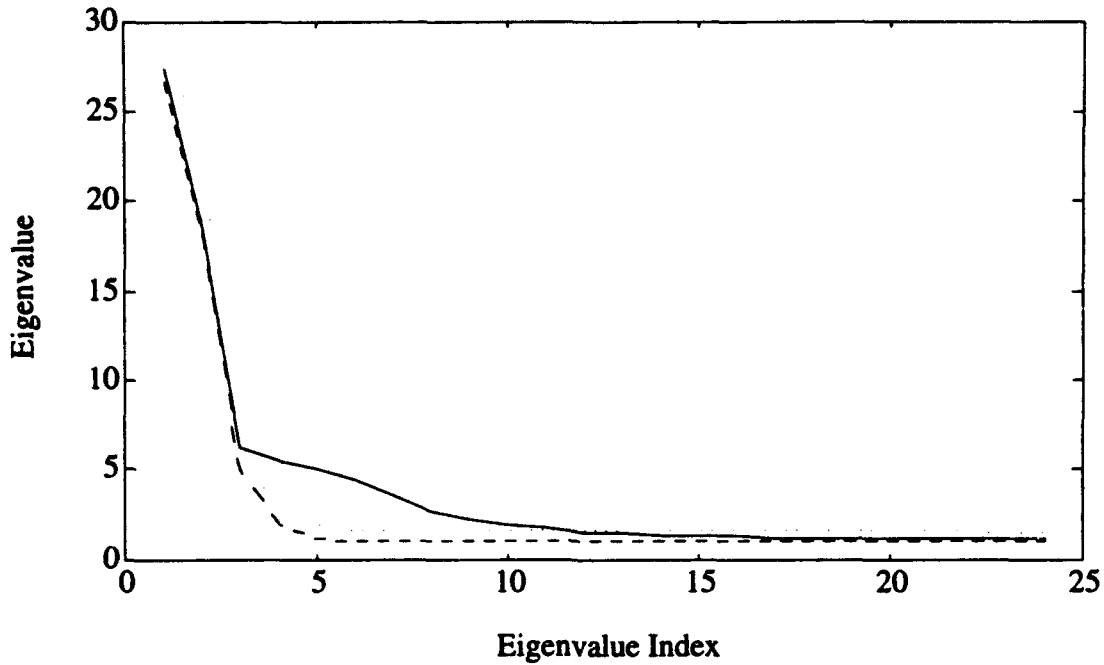


Figure 11. Eigenvalues of the STC

Table 2 shows the values of the likelihood functional for the various covariance structures. The magnitude of the likelihood functional directly relates to the size of the gradient and consequently to the convergence rate. While the first pass converged in about 10 iterations, attempts at modifying the step size for the second pass resulted in extremely slow convergence and, ultimately, algorithm failure.

Table 2. Values of Likelihood Functional for STC

	$L_q(\mathbf{Q}) = (N-q)(\ln(\bar{\lambda}_{GM}(q)) - \ln(\bar{\lambda}_{AM}(q)))$
$\mathbf{R} = \sigma_{DS}^2 \mathbf{P} + \sigma_{ES}^2 \mathbf{Q} + \sigma_0^2 \mathbf{I}_N$ (solid)	-0.5501
$\mathbf{R}_w = \mathbf{L}^{-1} \mathbf{R} \mathbf{L}^{-H}$ (dotted)	-0.0009442
$\mathbf{R} = \sigma_{DS}^2 \mathbf{P} + \sigma_0^2 \mathbf{I}_N$ (dashed)	0

To visualize the gradients involved, figure 12 depicts the likelihood functional of the STC as a function of the real and imaginary components of the primary AR coefficient. In this case, the

primary pole equals $-0.0044 - 0.6910i$, the maximum of the surface. Figure 13 represents a contour of the surface.

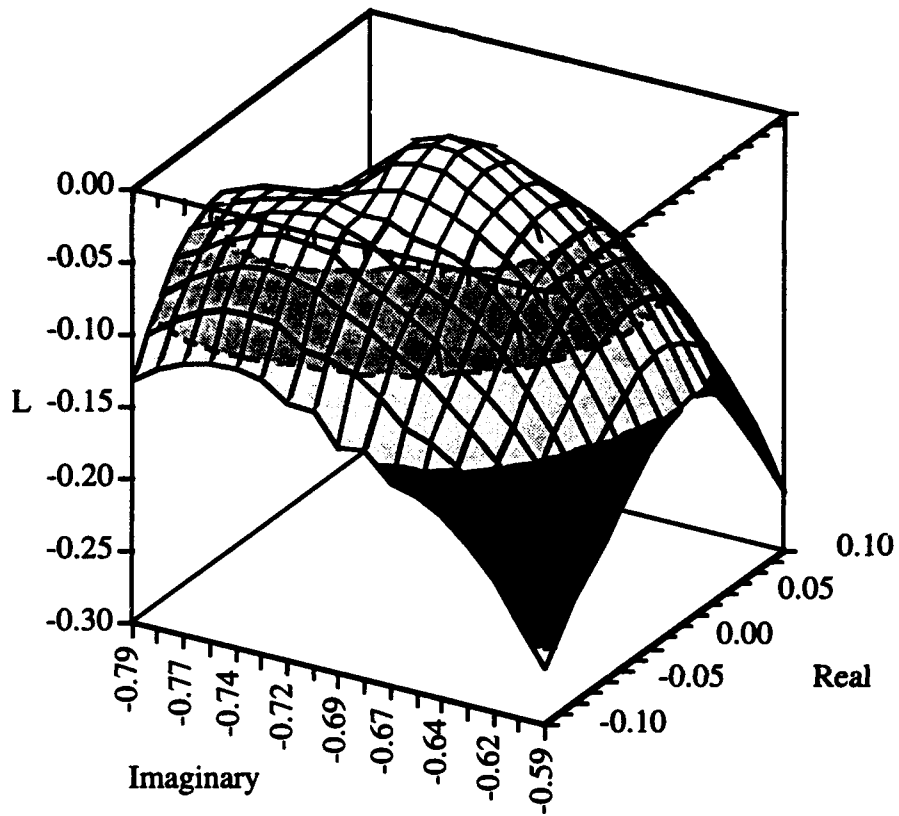


Figure 12. Likelihood Functional Surface for STC

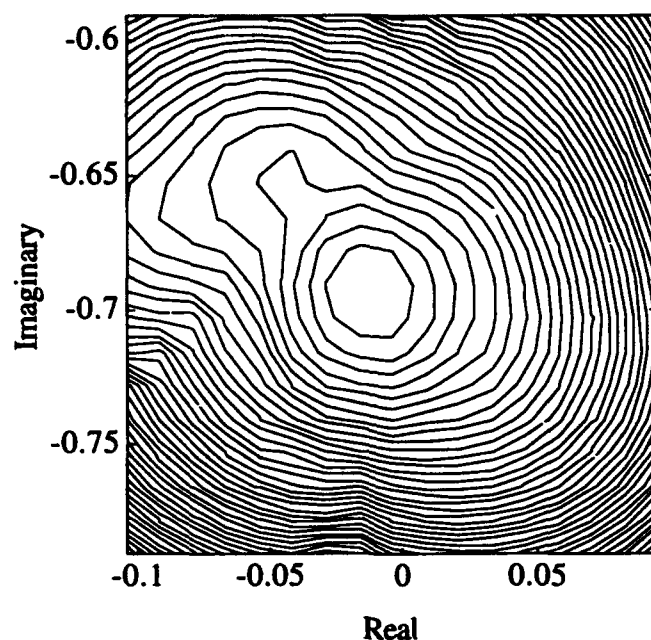


Figure 13. Likelihood Functional Contour for STC

A second interpretation of the failure of the second pass of the algorithm relies on the magnitude of the AR coefficient for the second extended source. The magnitude of the coefficient equals 0.96, close to the unit circle. As the AR coefficient moves closer to the unit circle, the Gohberg formula produces an extended source covariance with extreme ill-conditioning due to a very strong principal eigenvalue. Essentially this type of covariance models a discrete source. The source contributes only to the principal eigenvalues of the covariance \mathbf{R} . In this manner, the pre-whitening eigenvalues that appear after the principal eigenvalues remain unaffected, contributing to a flat white eigenvalue spectrum.

CONCLUSIONS

The STC emphasizes certain deficiencies of the Le Cadre¹¹ prewhitening technique.* The presence of multiple extended sources that comprise the spatially colored noise results in the greatest difficulty. The great disparity in SNR between the two extended sources causes the algorithm to concentrate almost solely on the stronger source. After prewhitening the first strong source, a promotion of the weaker source occurs using MUSIC, although the noise eigenvalues represent nearly a white noise spectrum. A second pass of the prewhitener fails due to the nature of the prewhitened eigenvalues. Although the results are not presented here, inaccurate knowledge of the noise floor σ_0^2 diminishes algorithm performance substantially.

The estimate of the number of sources present in the acoustic field also greatly affects algorithm performance. Since many problems in sensor array processing rely on this estimate, research into its computation actively continues.

All optimization problems based on gradient algorithms suffer from inaccurate initialization and computation of suitable step size. Indeed, Le Cadre¹¹ presents a method for step size updating and provides the algorithm starting point. Other suitable techniques for optimization exist for this type of problem, notably the Broyden-Fletcher-Goldfarb-Shanno routines.²⁷

The parametric assumptions on the noise model restrict the utility of this approach to nonuniform arrays. The AR formulation fails when inaccurate sensor spacing or a curvature exists in the line array. Future work will attempt to address these inadequacies. Recent related research includes the work of Kay and Nagesha.^{28, 29}

* The MATLAB source code in this report will be provided to any interested party by electronic media.

APPENDIX A: COMPUTATION OF $\frac{\partial Q^1}{\partial a_i}$

(Omit all unnecessary indexing for simplicity.)

Define the N by N matrices Z^i such that

$$Z^i(j, k) = \begin{cases} 1 & \text{if } j-k = i \quad 1 \leq j \leq N \\ 0 & \text{else} \quad 1 \leq k \leq N \end{cases} \quad (\text{A-1})$$

Write the Toeplitz matrices A_1 and A_3 as

$$\begin{aligned} A_1 &= \sum_{i=0}^L a_i Z^i = a_0 I_N + \sum_{i=1}^L a_i Z^i, \\ A_3 &= \sum_{i=1}^L a_i Z^{N-i}. \end{aligned} \quad (\text{A-2})$$

To simplify the computation, formulate A_1 and A_3 in vector form:

$$\begin{aligned} A_1 &= a_0 I_N + [a_1 \ a_2 \ \dots \ a_L] \begin{bmatrix} Z^1 \\ Z^2 \\ \vdots \\ Z^L \end{bmatrix} \\ &= a_0 I_N + \bar{\mathbf{a}}^T \bar{\mathbf{Z}}_1, \end{aligned} \quad (\text{A-3})$$

$$\begin{aligned} A_3 &= [a_1 \ a_2 \ \dots \ a_L] \begin{bmatrix} Z^{N-1} \\ Z^{N-2} \\ \vdots \\ Z^{N-L} \end{bmatrix} \\ &= \bar{\mathbf{a}}^T \bar{\mathbf{Z}}_2, \end{aligned} \quad (\text{A-4})$$

where " $\bar{\cdot}$ " emphasizes a vector variable. Express the complex coefficients a_i as the sum of real and imaginary parts x_i and y_i so that

$$\begin{aligned} a_0 &= x_0 + jy_0, \\ \bar{a} &= \bar{x} + j\bar{y}, \end{aligned} \quad (\text{A-5})$$

where $j = \sqrt{-1}$. With the Gohberg formula formulate the matrix Q as

$$\begin{aligned} Q^{-1} &= \frac{1}{\sigma_{ES}^2} (A_1 A_1^H - A_3 A_3^H) \\ &= \frac{1}{\sigma_{ES}^2} \left(\left\{ (x_0 + jy_0)I_N + (\bar{x}^T + j\bar{y}^T)\bar{Z}_1 \right\} \left\{ (x_0 - jy_0)I_N + \bar{Z}_1^T(\bar{x} - j\bar{y}) \right\} \right. \\ &\quad \left. - \left\{ (\bar{x}^T + j\bar{y}^T)\bar{Z}_2 \right\} \left\{ \bar{Z}_2^T(\bar{x} - j\bar{y}) \right\} \right). \end{aligned} \quad (\text{A-6})$$

First compute the partial derivatives with respect to the zero-th coefficient:

$$\begin{aligned} \frac{\partial Q^{-1}}{\partial x_0} &= \frac{1}{\sigma_{ES}^2} \left[\begin{array}{l} I_N \{ (x_0 - jy_0)I_N + \bar{Z}_1^T(\bar{x} - j\bar{y}) \} \\ + \{ (x_0 + jy_0)I_N + (\bar{x}^T + j\bar{y}^T)\bar{Z}_1 \} I_N \end{array} \right], \\ &= \frac{1}{\sigma_{ES}^2} \left[2x_0 I_N + \bar{Z}_1^T(\bar{x} - j\bar{y}) + (\bar{x}^T + j\bar{y}^T)\bar{Z}_1 \right], \\ &= \frac{1}{\sigma_{ES}^2} [A_1 + A_1^H], \end{aligned} \quad (\text{A-7})$$

$$\begin{aligned} \frac{\partial Q^{-1}}{\partial y_0} &= \frac{1}{\sigma_{ES}^2} \left[\begin{array}{l} jI_N \{ (x_0 - jy_0)I_N + \bar{Z}_1^T(\bar{x} - j\bar{y}) \} \\ + \{ (x_0 + jy_0)I_N + (\bar{x}^T + j\bar{y}^T)\bar{Z}_1 \} (-jI_N) \end{array} \right], \\ &= \frac{j}{\sigma_{ES}^2} \left[\begin{array}{l} (x_0 - jy_0)I_N + \bar{Z}_1^T(\bar{x} - j\bar{y}) - (x_0 + jy_0)I_N \\ - (\bar{x}^T + j\bar{y}^T)\bar{Z}_1 \end{array} \right], \\ &= \frac{j}{\sigma_{ES}^2} [A_1^H - A_1]. \end{aligned} \quad (\text{A-8})$$

Define the complex gradient³⁰ as

$$\begin{aligned} \frac{\partial Q^{-1}}{\partial a_0} &= \frac{\partial Q^{-1}}{\partial x_0} + j \frac{\partial Q^{-1}}{\partial y_0} \\ &= \frac{2}{\sigma_{ES}^2} A_1. \end{aligned} \quad (\text{A-9})$$

Compute the partial derivatives with respect to the first through the Lth coefficients:

$$\begin{aligned} \frac{\partial Q^{-1}}{\partial \bar{x}} &= \frac{1}{\sigma_{ES}^2} \left[\begin{array}{l} \bar{Z}_1 \{ (x_0 - jy_0) I_N + \bar{Z}_1^T (\bar{x} - j\bar{y}) \} \\ + \{ (x_0 + jy_0) I_N + (\bar{x}^T + j\bar{y}^T) \bar{Z}_1 \} \bar{Z}_1 \\ - \bar{Z}_2 (\bar{Z}_2^T (\bar{x} - j\bar{y})) - (\bar{x}^T + j\bar{y}^T) \bar{Z}_2 (\bar{Z}_2) \end{array} \right], \\ &= \frac{1}{\sigma_{ES}^2} [\bar{Z}_1 A_1^H + A_1 \bar{Z}_1 - \bar{Z}_2 A_3^H - A_3 \bar{Z}_2], \end{aligned} \quad (A-10)$$

$$\begin{aligned} \frac{\partial Q^{-1}}{\partial \bar{y}} &= \frac{1}{\sigma_{ES}^2} [j\bar{Z}_1 A_1^H - jA_1 \bar{Z}_1 - j\bar{Z}_2 A_3^H + jA_3 \bar{Z}_2], \\ &= \frac{j}{\sigma_{ES}^2} [\bar{Z}_1 A_1^H - A_1 \bar{Z}_1 - \bar{Z}_2 A_3^H + A_3 \bar{Z}_2], \end{aligned} \quad (A-11)$$

$$\begin{aligned} \frac{\partial Q^{-1}}{\partial \bar{a}} &= \frac{\partial Q^{-1}}{\partial \bar{x}^T} + j \frac{\partial Q^{-1}}{\partial \bar{y}^T}, \\ &= \frac{2}{\sigma_{ES}^2} [A_1 \bar{Z}_1^T - A_3 \bar{Z}_2^T]. \end{aligned} \quad (A-12)$$

The expressions in equations (A-10) - (A-13) also correctly compute the partial of the zero-th coefficient since

$$Z^0 = I_N \quad (A-13)$$

and

$$Z^N = 0_N. \quad (A-14)$$

APPENDIX B: SOURCE CODE FOR PREWHITENING ALGORITHM

```
% *****  
% This MATLAB program implements Le Cadre's algorithm for  
% estimating the noise covariance matrix B for the STC.  
  
% Author: Alain C. Barthelemy  
% Date: 23 June 1993  
% *****  
  
clear;  
clg;  
clc;  
disp('');  
hold off;  
axis('normal');  
  
% PARAMETERS FOR STANDARDIZED TEST CASE (STC)  
  
j = sqrt(-1); % Complex variable  
th = [45 70 85 90 105]; % Discrete source bearings  
vs = [0.02 0.515 0.23 0.23 0.005]; % Source variances  
varnoiz = 1; % Power of noise  
varsig = 2; % Power of signal  
ambnoiz = 1; % Power in ambient noise  
sp = 0.25; % Nominal sensor spacing  
N = 24; % Total Number of sensors  
thn = [0 135]; % DOA angles for extended sources  
% Complex AR coefficients  
a = [-0.7 -0.96].*exp(j*2*pi*sp*cos(thn*pi/180));  
  
alpha = [0.998 0.002]; % Weighting for 2 extended sources  
  
% PARAMETERS FOR PRE-WHITENING ALGORITHM  
p = 4; % Estimated order of AR process  
q = 7; % Estimate of the number of sources  
rho = -0.025; % Step size for gradient algorithm  
num_k = 25; % Maximum number of Le Cadre iterations  
  
% PARAMETERS FOR DISPLAY  
  
% [# circle divs, # polar lines, # circles]
```

```

gr_p   = [100 12 4];
theta  = linspace(0, 2*pi, gr_p(1));
phi    = linspace(0, 2*pi-((2*pi)/gr_p(2)), gr_p(2));
this   = ones(gr_p(1),1)*linspace(1/gr_p(3),1,gr_p(3));

% COMPUTE COVARIANCE STRUCTURE FOR STC

B01 = B_F(vernoiz, a(1), N);           % First extended source
B01 = (N/trace(B01))*B01;              % Normalize
B02 = B_F(vernoiz, a(2), N);           % Second extended source
B02 = (N/trace(B02))*B02;              % Normalize
B0   = alpha(1)*B01 + alpha(2)*B02;    % Scaled sum
% 5 discrete sources
DP   = exp(sqrt(-1)*2*pi*sp*[0:N-1]'*(cos(th*pi/180)));
P    = DP*diag(vs)*DP';                % Scaled
P    = (N/trace(P))*P;                  % Normalize
R    = varsig*P + vernoiz*B0 + ambnoiz*eye(N); % Covariance

% REMOVE DIAGONAL FROM R, ASSUME KNOWLEDGE OF NOISE FLOOR

R = R - ambnoiz*eye(N);

% R NOW CONTAINS SMALL IMAGINARY COMPONENTS ON ITS
% DIAGONAL MAKE R POSITIVE DEFINITE FOR CHOLESKY
% COMPUTATION, THIS DOES NOT ALTER R IN ANY SIGNIFICANT
% WAY

R = (R+R')/2;

% COMPUTE A YULE-WALKER APPROXIMATION OF THE POLE
% LOCATIONS, OF THE SUM OF THE TWO EXTENDED SOURCES

poles = B0(1:p, 1:p) \ (-B0(2:(p+1), 1));
B_poles = B_FI(vernoiz, poles, N);      % Use in cosine metric

% PRE-COMPUTE Z MATRICES

Z1 = zeros((p+1)*N, N);                % Initialize
Z2 = Z1;
for i = 0:p,
    Z1((1:N)+i*N, :) = Z_FUNC(i, N).';
    Z2((1:N)+i*N, :) = Z_FUNC(N-i, N).';
end;

```

```

% LE CADRE'S ALGORITHM FOR ESTIMATING THE COVARIANCE
% MATRIX B

A      = [1;zeros(p, 1)];           % Initialize parameter vector
T      = chol(R)';                 % Compute Cholesky factor of R
metric = zeros(num_k, 1);          % Initialize cosine metric
G      = zeros(p+1, 1);            % Initialize gradient
% Initialize matrix of estimated parameters
A_plot = zeros(num_k, (p+1));

for k = 1:num_k,                    % Iteration index

    A      = A - rho*G;              % Update parameter vector
    A_plot(k, :) = A.'; % Fill in matrix of estimated parameters
    % Form estimated covariance matrix B
    inv_B   = B_FI(A(1), A(2:(p+1)), N);

% COMPUTE PERFORMANCE METRIC

    metric(k) = ...
    real(trace(inv_B*B_poles)/sqrt(trace(B_poles*B_poles)* ...
    trace(inv_B*inv_B)));

% CALCULATION OF GRADIENT VECTOR G REQUIRES KNOWLEDGE OF
% THE EIGENSTRUCTURE OF T'*INV(B)*T

    [U, LAM] = eig(T'*inv_B*T);      % Compute eigenstructure
    % Vector of small eigenvalues
    LAM      = diag(LAM(q+1:N, q+1:N));
    ar       = mean(LAM); % Arithmetic mean of small eigenvalues

% UPDATE OF GRADIENT VECTOR G

    for i = 0:p,                    % Index over AR coefficients

        % PARTIAL DERIVATIVES OF INV(B) RELATIVE TO A SUB I

        deli = (2/A(1))*(A1_F(A(2:(p+1)), N)*Z1((1:N)+i*N, :) ...
        - A3_F(A(2:(p+1)), N)*Z2((1:N)+i*N, :));

        % DERIVATIVE MATRICES

```

```

    deliprime = T'*deli*T;

% PARTIAL DERIVATIVES OF THE EIGENVALUES OF PRE-WHITENED R

    partial = diag(U(:, q+1:N) '*deliprime*U(:, q+1:N));

% UPDATE OF GRADIENT VECTOR G

    G(i+1) = sum(partial./LAM) - sum(partial)/ar;

end;

end;

% SET UP DISPLAY GRAPH AND POLE PLOT

axis('square');                % Set aspect ratio to square
axis([-1 1 -1 1]);            % Set coordinate axes

% PLOT POLE PLOT

plot(real(poles), imag(poles), 'clo', [zeros(gr_p(2), 1) ...
cos(phi)']', [zeros(gr_p(2), 1) sin(phi)']', 'cl:', ...
this.*(ones(gr_p(3),1)*cos(theta))', this.* ...
(ones(gr_p(3),1)*sin(theta))', 'cl:', ...
real(A_plot(:, 2:(p+1))), imag(A_plot(:, 2:(p+1))), 'clx');

xlabel('Real');                % Label x axis
ylabel('Imaginary');          % Label y axis

pause;                          % Pause in execution

% PLOT COSINE METRIC

axis('normal');                % Set aspect ratio to default
% Size coordinate axes
axis([1 num_k min(metric) max(metric)]);

% PLOT METRIC

plot(1:num_k, metric, 'cl-');

```

```

grid; % Put grid onto graph
xlabel('Iteration number'); % Label x axis
ylabel('Cosine metric'); % Label y axis

pause; % Pause in execution

% COMPUTE AND PLOT NOISE SPATIAL DENSITIES

M = 301; % Number of bearing bins
% Angles from 0 to 180 degrees
degree_angles = linspace(0, pi, M);
bearing_angles = cos(degree_angles); % Cosine of above
psd_plot = zeros(M, num_k); % Initialize for plotting

for k = 1:num_k, % Iteration index

    % COMPUTE NOISE SPATIAL DENSITY

    psd_plot(:, k) = ARMA([1 A_plot(k, 2:(p+1))], 1, ...
        degree_angles, sp).';

    % ADD ARBITRARY FACTOR FOR DISPLAY PURPOSES

    psd_plot(:, k) = psd_plot(:, k) + (k*3);

end;

axis([1 2 3 4]); axis; % Set axes scaling to automatic

% PLOT NOISE SPATIAL DENSITY

plot(bearing_angles, psd_plot, 'c1-');

xlabel('cos(bearing)'); % Label x axis
ylabel('Iteration ->'); % Label y axis

pause; % Pause in execution

% COMPUTE AND PLOT MUSIC RESPONSES

e = 1e+16; % Enhancement factor for signal subspace
DS = exp(-sqrt(-1)*2*pi*sp*(0:N-1)).'...
*cos(0:(pi/(M-1)):pi)); % Steering matrix

```

```

num_src = q; % Assumed number of sources for MUSIC
br_plot = zeros(M, num_k); % Initialize bearing response plot

for k = 1:num_k, % Iteration index

    % FORM ESTIMATED NOISE COVARIANCE MATRIX B

    B_EST = B_F(A_plot(k, 1), A_plot(k, 2:(p+1)).', N);
    B_EST = (N/trace(B_EST))*B_EST; % Normalize
    % Make positive definite for Cholesky
    B_EST = (B_EST+B_EST')/2;

    L = chol(B_EST)'; % Compute Cholesky factor

    % FORM PRE-WHITENED ESTIMATE OF R

    RW = inv(L)*R*inv(L');

    % ADD NOISE FLOOR BACK IN

    RW = RW + ambnoiz*eye(N);

    [U, LAM, AA] = svd(RW); % Compute eigenstructure of RW
    LAM = diag(LAM); % Vector of eigenvalues

    % COMPUTE MUSIC BEARING RESPONSE

    br_plot(:, k) = ...
    real([sum(DS.*((eye(N)-U(:, (1:num_src)))*...
    diag(e*(LAM(1:num_src)-1)./(1+e*(LAM(1:num_src)-1)))...
    *U(:, (1:num_src))'))*conj(DS))])'. \ (N*N*ones(M,1));

    % NORMALIZE RESPONSE, CONVERT TO DB

    br_plot(:, k) = 10.*log10(br_plot(:, k)./max(br_plot(:, k)));

    % ADD FACTOR TO EACH RESPONSE FOR DISPLAY PURPOSES

    br_plot(:, k) = br_plot(:, k) + (k*20);

end;

% PLOT MUSIC BEARING RESPONSES

```

```

plot(bearing_angles, br_plot, 'c1-');

xlabel('cos(bearing)');           % Label x axis
ylabel('Iteration ->');         % Label y axis

% *****
% FUNCTIONS - MUST BE UTILIZED AS SEPARATE M-FILES
% *****

function y = A1_F(a, N);

% COMPUTES THE MATRIX A1

    y = toeplitz([1;a;zeros((N-length(a)-1), 1)], ...
[1 zeros(1, N-1)]);

return;

% *****

function y = A3_F(a, N);

% COMPUTES THE MATRIX A3

    y = toeplitz([zeros(N-length(a), 1);flipud(a)], zeros(1, N));

return;

% *****

function y = ARMA(a, b, theta, sp);

% COMPUTES SPATIAL DENSITY OF AN ARMA(P, Q) PROCESS ACROSS
% BEARINGS SPECIFIED BY THETA, AND AT SENSOR SPACING SP

    p = length(a);           % AR order
    q = length(b);           % MA order
    M = length(theta);       % Number of bearing bins
    z = exp(-sqrt(-1)*2*pi*sp*cos(theta));

    A = a*[[ones(p, 1)*z].^[[0:1:(p-1)].']*ones(1, M)]; % A(z)
    B = b*[[ones(q, 1)*z].^[[0:1:(q-1)].']*ones(1, M)]; % B(z)

```

```

    y = (B.*conj(B))./(A.*conj(A));           % Spatial density

return;

% *****

function y = B_F(vernoiz, a, N);

% COMPUTES COVARIANCE MATRIX BASED ON THE GOHBERG
% FORMULATION

    A1 = A1_F(a, N);                         % Compute matrix A1
    A3 = A3_F(a, N);                         % Compute matrix A3

    % True noise covariance matrix
    y = inv((1/vernoiz)*(A1*A1' - A3*A3'));

return;

% *****

function y = B_FI(vernoiz, a, N);

% COMPUTES INVERSE COVARIANCE MATRIX BASED ON THE
% GOHBERG FORMULATION

    A1 = A1_F(a, N);                         % Compute A1 matrix
    A3 = A3_F(a, N);                         % Compute A3 matrix

    % Inverse of true noise covariance matrix
    y = (A1*A1' - A3*A3')/vernoiz;

return;

% *****

function y = Z_FUNC(i, N);
% COMPUTES THE Z(I) MATRIX
    y      = zeros(N);
    j_matrix = (1:N).'*ones(1,N);
    this    = find((j_matrix-j_matrix.') == i);
    y(this) = ones(1, length(this));

return;

```

REFERENCES

1. R. O. Schmidt, "Multiple Emitter Location and Signal Parameter Estimation," reprinted in *IEEE Transactions on Antennas Propagation*, vol. AP-34, March 1986.
2. N. L. Owsley, "Enhanced Minimum Variance Beamforming," in *Underwater Acoustic Data Processing*, Editor Y. Chan, NATO ASI Series, Kluwer, 1989.
3. R. Kumaresan and D. W. Tufts, "Estimating the Angles of Arrival of Multiple Plane Waves," *IEEE Transactions on AES*, vol. AES-19, no. 1, January 1983.
4. A. J. Barabell, "Improving the Resolution Performance of Eigenstructure-Based Direction-Finding Algorithms," in *Proc. of ICASSP*. 1983.
5. R. Roy and T. Kailath, "ESPRIT - Estimation of Signal Parameters Via Rotational Invariance Techniques," *IEEE Transactions on ASSP*, vol. 37, no. 7, July 1989.
6. V. F. Pisarenko, "The Retrieval of Harmonics from a Covariance Function," *Geophys. Jour. Roy. Astr. Soc.*, Vol. 33, 1973.
7. A. H. Tewfik, "Direction Finding in the Presence of Colored Noise by Candidate Identification," *IEEE Transactions on SP*, vol. 39, no. 9, September 1991.
8. N. L. Owsley, "A Comparison of Spatial Signal Processors With Realistic Data," *NATO/ASI Conference, Acoustic Signal Processing for Ocean Exploration, Madeira, Portugal, 27 July 1992*.
9. N. L. Owsley, "A Standardized Test Case (STC) for Sensor Array Processor Evaluation," *IEEE Oceans '91 Conference, Honolulu, Hawaii, 30 September 1991*.
10. T. Kailath, A. Vieira and M. Morf, "Inverse of Toeplitz Operators, Innovations and Orthogonal Polynomials," *SIAM Review*, vol. 20, January 1978, pp. 106-119.
11. J. P. Le Cadre, "Parametric Methods for Spatial Signal Processing in the Presence of Unknown Colored Noise Fields," *IEEE Transactions on ASSP*, vol. 37, no. 7, July 1989.

12. S. M. Kay and S. L. Marple, "Spectrum Analysis - A Modern Perspective," *IEEE Proceedings*, vol. 69, no. 11, Nov. 1981.
13. M. Wax and T. Kailath, "Detection of Signals by Information Theoretic Criteria," *IEEE Transactions on ASSP*, vol. ASSP-33, no. 2, April 1985.
14. H. Akaike, "A New Look at the Statistical Model Identification," *IEEE Transactions on Automatic Control*, vol. AC-19, December 1974.
15. J. Rissanen, "A Universal Prior for the Integers and Estimation by Minimum Description Length," *Annals of Statistics*, vol. 11, 1983.
16. A. C. Barthelemy and N. L. Owsley, "Sensor Array Processor Evaluation With a Standardized Test Case (STC)," *IEEE Twenty-fifth Annual Asilomar Conference on Signals, Systems and Computers*, Pacific Grove, California, 5 November 1991.
17. J. F. Yang and M. Kaveh, "Adaptive Eigensubspace Algorithms for Direction or Frequency Estimation and Tracking," *IEEE Transactions on ASSP*, vol. 36, no. 2, February 1988.
18. R. Schreiber, "Implementation of Adaptive Array Algorithms," *IEEE Transactions on ASSP*, vol. 34, no. 5, Oct. 1986.
19. I. Karasalo, "Estimating the Covariance Matrix by Signal Subspace Averaging," *IEEE Transactions on ASSP*, vol. 34, no. 1, February 1986.
20. N. L. Owsley, "Adaptive Data Orthogonalization," *Proceedings of ICASSP 1978*.
21. D. W. Tufts and C. D. Melissinos, "Simple, Effective Computation of Principal Eigenvectors and Their Eigenvalues and Application to High-Resolution Estimation of Frequencies," *IEEE Transactions on ASSP*, vol. 34, no. 5, October 1986.
22. P. Comon and G. Golub, "Tracking a Few Extreme Singular Values and Vectors in Signal Processing," *IEEE Proceedings*, vol. 78, no. 8, August 1990.

23. R. D. DeGroat and R. A. Roberts, "Efficient, Numerically Stabilized Rank-One Eigenstructure Updating," *IEEE Transactions on ASSP*, vol. 38, no. 2, February 1990.
24. R. D. DeGroat, "Noniterative Subspace Tracking," *IEEE Transactions on SP*, vol. 40, no. 3, March 1992.
25. B. Champagne, "Adaptive Eigendecomposition of Data Covariance Matrices Based on First-Order Perturbations," *submitted for publication to IEEE Transactions on SP*, February 1993.
26. L. Marple, *Digital Spectral Analysis with Applications*, Prentice-Hall Signal Processing Series, Englewood Cliffs, NJ, 1987.
27. D. G. Luenberger, *Linear and Nonlinear Programming*, Addison-Wesley Publishing Company, Reading, MA, 1984.
28. S. Kay and V. Nagesha, "Estimation for Processes with Mixed Spectra," in *Proc. ICASSP*, pp. IV-232-235, 1993.
29. V. Nagesha and S. Kay, "Maximum Likelihood Estimation for Array Processing in Colored Noise," in *Proc. ICASSP*, pp. IV-240-243, 1993.
30. S. Kay, *Modern Spectral Estimation: Theory & Application*, Prentice-Hall, Englewood Cliffs, NJ, 1988.

INITIAL DISTRIBUTION LIST

Addressee

No. of Copies

DTIC

12